

AN EFFICIENT ALGORITHM FOR CHEMICAL POTENTIAL COMPUTATION OF ANISOTROPIC SYSTEMS

Habtamu Zewdie

Department of Chemistry, Addis Ababa University
P.O. Box 1176, Addis Ababa, Ethiopia

(Received May 17, 1990; revised September 29, 1990).

ABSTRACT. Techniques of computing the chemical potential via computer simulation from a canonical ensemble are developed for the special case of lattice systems with periodic boundary conditions. An exactly solvable model is used to test the predictions of the techniques. It is shown that the particle insertion method used gives a better recipe for Monte Carlo sampling from a canonical ensemble of anisotropic systems. Good results have been obtained over a wide range of temperatures for the entropy and the chemical potential. Size dependent structural and thermodynamic properties are identified.

INTRODUCTION

The computation of the chemical potential and entropy for a model system by computer simulation methods are more difficult than for mechanical or other thermal properties (1-7). Computation of the chemical potential has been attempted by integrating the equation of state at constant temperature, which has many disadvantages (8,9), or by using the grand canonical ensemble (GCE) Monte Carlo (MC) method (10-12), which requires a special programme. Adams (13) has used the Widom method (14,15) for hard spheres for MC. The Widom method has also been used to calculate the entropy and vapour pressure using MC by Romano and Singer (16). The same method, and data, were used by Powles (17) to calculate the coexistence line for liquids resembling chlorine and bromine. Svensson and Woodward (18) have also developed and applied Widom's method to study electrolyte solutions. A complimentary method to Widom's which has considerable advantages, especially for the study of solutions, has been shown by Shing and Gubbins (19), a different approach is also followed by Torrie and Valeau (20) to estimate the chemical potential of a fluid by sampling on distributions designed for this purpose, rather than on the usual Boltzmann distribution. However, this method has the difficult problem of designing a suitable distribution. The objects of this paper are:-

1. To test the existing procedures for chemical potential computation from a canonical ensemble against predictions of an exactly solvable model.
2. To propose an efficient algorithm for chemical potential computation from canonical ensemble of anisotropic systems restricted to lattice sites and allowed to interact only to nearest neighbours.

THE MODEL

The system we have chosen belongs to the Lebwohl-Lasher (21) model family and is defined by the hamiltonian

$$U_N = (1/2) \sum_{i=1}^N \sum_{j=1}^N u_{ij}, \quad i \neq j \quad (1)$$

where

$$u_{ij} = -\varepsilon_{ij} \cos(2\beta_{ij}), \quad (2)$$

and N is the number of particles. The particles are confined to a plane containing the line of centres and taken to be on a regular one dimensional lattice. β_{ij} measures the angle between the symmetry axes of molecules i and j . ε_{ij} designates the strength of attractive interactions between molecules i and j . Here $\varepsilon_{ij} = \varepsilon$ if i and j are nearest neighbours and 0 otherwise. Cyclic boundary conditions are assumed. In the thermodynamic limit, when N tends to infinity, configurational contributions to the internal energy, specific heat, entropy per particle and chemical potential are given by (22,23)

$$U/N\varepsilon = -I_1(\varepsilon/kT)/I_0(\varepsilon/kT), \quad (3)$$

$$C_V/Nk = \frac{1}{2}(\varepsilon/kT)^2 \left\{ 1 + \frac{I_2(\varepsilon/kT)}{I_1(\varepsilon/kT)} - 2 \left(\frac{I_1(\varepsilon/kT)}{I_0(\varepsilon/kT)} \right)^2 \right\}, \quad (4)$$

$$S/Nk = \ln\{2\pi I_0(\varepsilon/kT)\} - (\varepsilon/kT) \frac{I_1(\varepsilon/kT)}{I_0(\varepsilon/kT)}, \quad (5)$$

$$\mu = -kT \ln\{2\pi I_0(\varepsilon/kT)\}. \quad (6)$$

The symbol $I_n(\varepsilon/kT)$ denotes an n^{th} order modified Bessel function. Since the chemical potential is a smooth function of temperature, this guarantees the absence of phase transitions at any finite temperature for the infinite system.

CHEMICAL POTENTIAL EXPRESSIONS

The configurational partition function for a system of N interacting particles at an absolute temperature T is

$$Z_N = \int_0^{2\pi} \dots \int_0^{2\pi} \exp\{-U_N/kT\} d\beta_1 \dots d\beta_N, \quad (7)$$

where k is the Boltzmann constant, $d\beta_1 \dots d\beta_N$ is a volume element in the configuration space of the N particles and U_N is the configurational potential energy defined by equations (1) and (2).

The chemical potential, μ , is the derivative of the Helmholtz free energy with respect to the number of particles

$$\mu = (\partial A / \partial N)_T \quad (8)$$

where

$$A = -kT \ln Z_N. \quad (9)$$

Differentiation of A with respect to a natural number, at least for large N , gives

$$\mu = -kT \ln(Z_N/Z_{N-1}), \quad (10)$$

$$= -kT \ln(Z_{N+1}/Z_N). \quad (11)$$

The chemical potential can be calculated in two different but in principle equivalent procedures. Next, brief descriptions of these procedures will be given.

Particle removing method. The N particle configurational partition function

is given by equation (7). It can be written as

$$Z_N = \int_0^{2\pi} \dots \int_0^{2\pi} \exp\{-(-\psi + U_{N+1})/kT\} d\beta_1 \dots d\beta_N, \quad (12)$$

$$= \frac{Z_{N+1}}{2\pi} < \exp(\psi/kT) >_{N+1}. \quad (13)$$

Rearranging equation (13) gives

$$Z_N/Z_{N+1} = < \exp(\psi/kT) >_{N+1} / 2\pi. \quad (14)$$

Here ψ is the work that would be done in removing a particle from the system to infinity. $< \dots >_{N+1}$ implies thermal average taken over all possible configurations of $N+1$ particles. Thus

$$\mu = kT \ln \{ < \exp(\psi/kT) >_{N+1} / 2\pi \}. \quad (15)$$

This is formally equivalent to Shing's result.

Particle insertion method. The particle inserted must, on the average, satisfy the equilibrium single particle thermodynamic properties of the system. Imagine that a fictitious particle with randomly chosen orientation is inserted at a randomly chosen position of the system. In doing so the fictitious particle measures the energy of interaction ψ , which is the work that would be done in bringing a particle from infinity to the chosen position in the system. We can, therefore, write

$$Z_{N+1} = \int_0^{2\pi} \dots \int_0^{2\pi} \exp\{-(\psi + U_N)/kT\} d\beta_1 \dots d\beta_{N+1}, \quad (16)$$

which leads to

$$Z_{N+1}/Z_N = 2\pi < \exp(-\psi/kT) >_N. \quad (17)$$

Thus the expression for the chemical potential would be

$$\mu = -kT \ln \{ 2\pi < \exp(-\psi/kT) >_N \}. \quad (18)$$

This is formally equivalent to Widom's method. Equation (14) is the inverse of equation (17). Therefore,

$$< \exp(-\psi/kT) >_N < \exp(\psi/kT) >_{N+1} = 1. \quad (19)$$

Computational details. We have studied a system of 250 particles which is known to give good results on most thermodynamic properties (24). A standard Monte Carlo Metropolis method with periodic boundary conditions has been employed to generate equilibrium configurations. The simulation was performed for 16 different scaled temperatures between $T^* = 0.1$ and $T^* = 2.0$ which include the heat capacity bump, where $T^* = kT/\epsilon$. The simulation at the lowest temperature studied has been started from a completely aligned system. The simulations at the other temperatures have been run in sequence starting from the equilibrium configurations at the nearest lower temperatures. A configuration of the system is defined by a set of N orientations $\{\beta_i\}$. A new configuration is generated by sequentially choosing a particle. A new trial orientation of the chosen particle is then generated using the controlled increment technique of Barker and Watts (25). In every simulation a minimum of 5000 cycles, where a cycle is a set of N attempted moves, have been used for equilibration and 5000 cycles were also found to be adequate for the production stage.

Computation of the chemical potential via particle removing method begins by evaluating ψ , the energy of interaction of any one of the real particles. However, ψ for site i changes only three times in a cycle. It is, therefore, sufficient to calculate $\psi(i)$ for $i = 1, N$ which is used to calculate $\exp(\psi/kT)$ once every cycle. This is then averaged over 500 cycles, which is defined to be a macrocycle, and the chemical potential determined at the end of each macrocycle from equation (15) which in terms of scaled quantities becomes

$$\mu^* = T^* \ln \{ \langle \exp(\psi^*/T^*) \rangle_{N+1} / 2\pi \}$$

where $\mu^* = \mu/\epsilon$, and $\psi^* = \psi/\epsilon$. (20)

As we have seen the chemical potential may also be obtained via the particle insertion method. At the end of each cycle two nearest-neighbour-real-particle positions are chosen sequentially and the fictitious particle is inserted with random orientation. ψ , the energy of interaction of the fictitious particle with its nearest neighbours, is calculated which is used to evaluate $\exp(-\psi/kT)$. $\exp(-\psi/kT)$ is summed over all possible positions and orientations of the fictitious particle for a given configuration of the system. This is repeated at the end of each cycle to calculate the desired average $\langle \exp(-\psi/kT) \rangle$ for a macrocycle. The chemical potential is then calculated via equation (18) which in reduced units becomes

$$\mu^* = -T^* \ln \{ 2\pi \langle \exp(-\psi^*/T^*) \rangle_N \}. \quad (21)$$

In principle a large number of random orientations could be assigned for the fictitious particle at the chosen position for a given configuration of the system to improve the results. This is one particular advantage of particle insertion method. In this work it is found sufficient to generate only one orientation per chosen position for each cycle.

The product $\langle \exp(\psi/kT) \rangle_{N+1} \langle \exp(-\psi/kT) \rangle_N$ is calculated at the end of each macrocycle. This result is used to identify the temperature range over which equation (19) holds.

The internal energy, U , is also calculated as

$$U = \langle U_N \rangle, \quad (22)$$

where U_N is the configurational potential energy given by equations (1) and (2). This quantity is of interest because it provides a more detailed test of the procedure on the scaled entropy per particle $S^*(\equiv S/Nk)$ together with the chemical potential via

$$S^* = (\overline{U^*} - \mu^*)/T^*, \quad (23)$$

where $\overline{U^*}(\equiv U/N\epsilon)$ is the scaled internal energy per particle.

An estimate of the errors in the various averages was obtained by dividing the production run into ten macrocycles, an average was calculated for each macrocycle and the standard deviation of these ten averages determined from

$$\sigma_X = \sqrt{\frac{1}{n(n-1)} \sum_{i=1}^n (\overline{X} - X_i)^2}, \quad (24)$$

where in this particular case $n = 10$, \overline{X} is the overall average for the n macrocycles and X_i is the average for quantity X over the i^{th} macrocycle. The system size dependence of the results were checked by repeating the simulation for system size of up to 10,000 particles at $T^* = 0.1$ where there is a maximum disagreement between the results of the two methods of computing the chemical potential.

RESULTS AND COMPARISON WITH THE THEORETICAL PREDICTIONS

Here, we begin by presenting the results for the chemical potential obtained via equations (20) and (21). We shall use the exact results for the model given by equation (6) for comparison. The variation of the scaled chemical potential with the scaled temperature is shown in Fig. 1. The results obtained via equation (20), shown as circles, is seen to agree with the predictions of the theory, shown

as a solid line, over a wide range of temperatures. Deviation between theory and simulation results obtained via equation (20) are observed at temperatures below $T^* \sim 0.3$ where the correlation length is significant compared with the size of the system.

A better agreement between exact results and that obtained via equation (21), shown as stars, is observed over all the temperature range studied. The errors in the computed chemical potentials are found to be very small and are less than the size of the points on the graph. The system size dependence of these results were tested by repeating the simulation for system size of up to 10,000 particles at $T^* = 0.1$. The results are found to agree within the statistical error.

Another view of this result can be obtained by plotting the scaled entropy per particle calculated via equation (23) at different temperatures (see Fig. 2). The particle insertion method gives a better estimate of the entropy (shown as stars). This is found to be in good accord with the predictions of the theory shown as a curve. The estimate of the entropy via the particle removing method, shown as circles in the Figure, is found to be good at high temperatures. However, at low temperatures the entropy is badly estimated and the errors associated with the averages are large. This may be due to strong correlation effects at low temperatures.

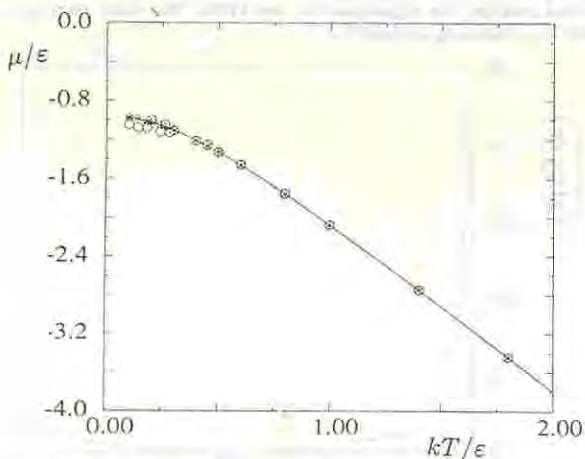


Fig. 1. The temperature dependence of the chemical potential. The curve indicates the exact results from equation (6). The symbols are simulation results: circles are from particle removing method via equation (20) and stars are from particle insertion method via equation (21).

In Fig. 3 the second rank orientational correlation function, $\overline{G_2(r_{ij}^*)} - \overline{\cos 2\beta_{ij}}$, where $r_{ij}^* = r_{ij}/a$ and a is the lattice parameter is presented. $\overline{G_2(r_{ij}^*)}$ for the model we have studied has two known properties, $\overline{G_2(r_{ij}^*)} = U/N\epsilon$ if i and j are nearest neighbours and $\lim_{r_{ij} \rightarrow \infty} \overline{G_2(r_{ij}^*)} \rightarrow 0$. However, $\overline{G_2(r_{ij}^*)}$ for $T^* = 0.1$ shown as dashed line levels off to ~ 0.09 implying a finite long-range orientational order at all finite temperatures. This behaviour is mimicked by the system for $T^* \sim 0.3$. $\overline{G_2(r_{ij}^*)}$ at $T^* = 0.3$ is shown as solid line. The product $\langle \exp(\psi/kT) \rangle N + 1 \langle \exp(-\psi/kT) \rangle N$ provides an alternative root to check the

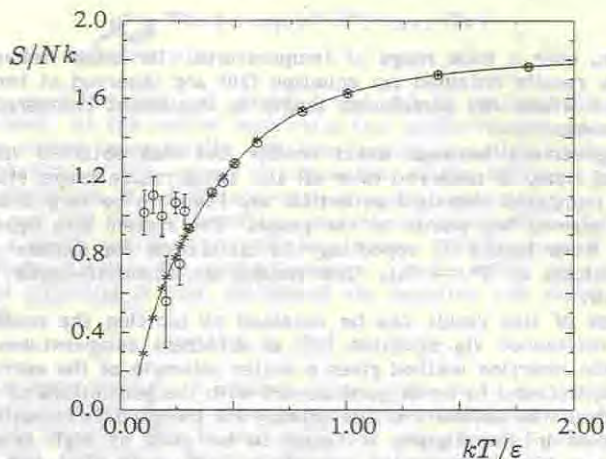


Fig. 2. Entropy versus temperature. The curve is analytical result (equation (5)), simulation results are indicated by symbols: circles from particle removing method (via equations (20) and (23)) and stars from particle insertion method (via equations (21) and (23)). The error bars are of length $2\sigma_S$, where $\sigma_S = -\sigma_{\mu^*}/T^*$.

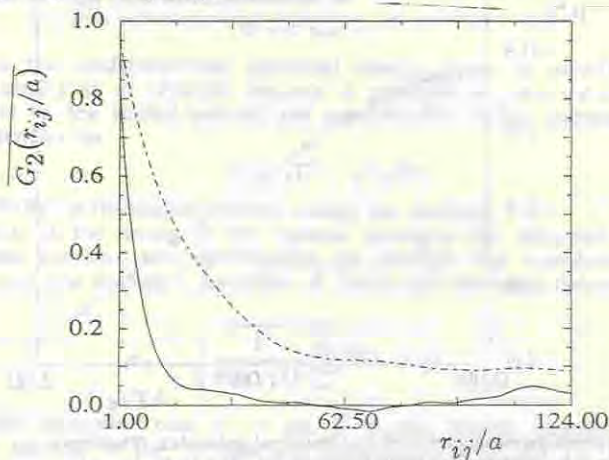


Fig. 3. The second rank orientational correlation function $\overline{G_2}(r_{ij}/a)$ as a function of scaled particle separation r_{ij}/a . The dashed line is for $kT/\epsilon = 0.3$.

above statements. The results are presented in Fig. 4. The solid line represents prediction of theory (equation (19)) and simulation results are presented as stars. Again an agreement between theory and simulation results hold above $T^* \sim 0.3$ where the long range order is ~ 0 . Properties such as internal energy (see Fig. 5) and the chemical potential calculated via particle insertion method and the corresponding entropy are found to be insensitive to the finite but small long-long order of the system.

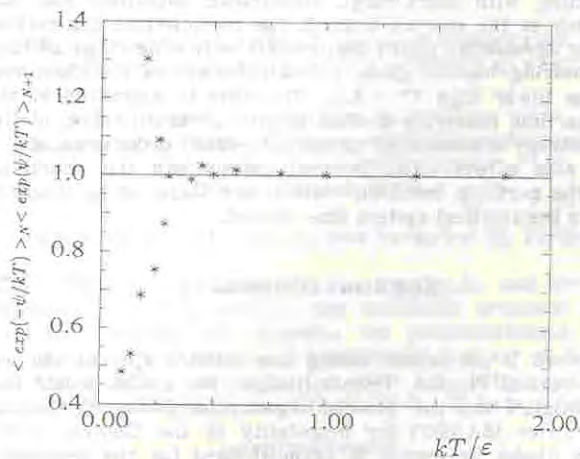


Fig. 4. The solid line is theoretical prediction (equation (19)) and the stars are simulation results.

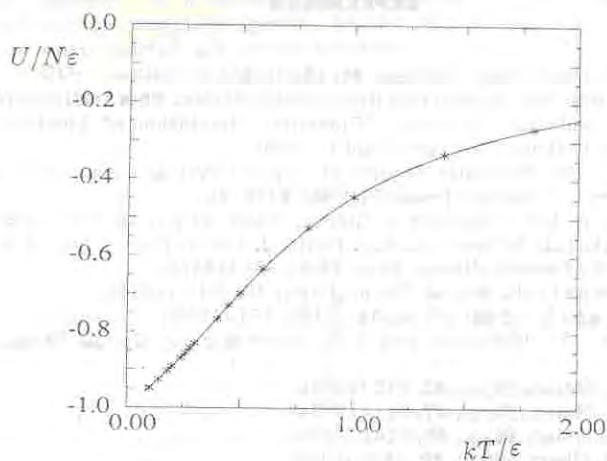


Fig. 5. The internal energy versus temperature. The solid line is prediction of theory (equation (3)) and the stars are simulation results.

CONCLUSION

Chemical potential is the most difficult property to estimate in molecular simulations. The analysis used in this work provides a reliable test of the two methods of chemical potential computations from canonical ensemble. For

systems interacting with short-range anisotropic potentials and restricted to lattice sites, such as the one we studied, the particle insertion method is found to be in a better agreement with exact results over wide range of temperatures. The particle removing method gives a bad estimate of the chemical potential for temperatures lower than $T^* \sim 0.3$. The error is magnified in the entropy. The failure of particle removing method to give accurate values of the chemical potentials and entropy is associated to the long-range order present in the system due the finite size effect. The internal energy and the chemical potential calculated via the particle insertion method are found to be insensitive to the sample size up to the smallest system size studied.

ACKNOWLEDGEMENTS

Part of this work is performed during the author's stay at the International Centre for Theoretical Physics, Trieste (Italy). The author would like to thank Professor Abdus Salam and the Swedish Agency for Research Cooperation with Developing Countries (SAREC) for hospitality at the Centre. The Computer Centre of Addis Ababa University is acknowledged for the generous allocation of computer time to this work. The author would also like to thank Dr. Theodoros Solomon for helpful discussions.

REFERENCES

1. J.G. Powles, *Chem. Phys. Letters*, **86**, 335 (1982).
2. G.R. Luckhurst, T.J. Sluckin and H.B. Zewdie, *Molec. Phys.*, **59**, 657 (1986).
3. M.P. Allen and D.J. Tildesley, "Computer Simulation of Liquids", Oxford Science Publications, Chapters 2 and 7 (1989).
4. C. Zannoni, "The Molecular Physics of Liquid Crystals" (eds. G.R. Luckhurst and G.W. Gray, Academic Press) Chapter 9 (1979).
5. J.G. Powles, W.A.B. Evans and N. Quirke, *Molec. Phys.*, **46**, 1347 (1982).
6. G.L. Deitrick, L.E. Scriven and H.T. Davis, *J. Chem. Phys.*, **90**, 2370 (1989).
7. B. Smit and D. Frenkel, *Molec. Phys.*, **68**(4), 951 (1989).
8. W.G. Hoover and F.H. Ree, *J. Chem. Phys.*, **49**, 3609 (1968).
9. J.P. Hansen and L. Verlet, *Phys. Rev.*, **184**, 151 (1969).
10. L.A. Rowley, D. Nicholson and N.G. Parsonage, *J. Comp. Phys.*, **17**, 401 (1975).
11. D.J. Adams, *Molec. Phys.*, **32**, 647 (1976).
12. D.J. Adams, *Molec. Phys.*, **37**, 211 (1979).
13. D.J. Adams, *Molec. Phys.*, **28**, 1241 (1974).
14. B. Widom, *J. Chem. Phys.*, **39**, 2808 (1963).
15. B. Widom, *J. Phys. Chem.*, **86**, 869 (1982).
16. S. Romano and K. Singer, *Molec. Phys.*, **37**, 1765 (1979).
17. J.G. Powles, *Molec. Phys.*, **41**, 715 (1980).
18. B.R. Svensson and C.E. Woodward, *Molec. Phys.*, **64**, 1247 (1988).
19. K.S. Shing and K.E. Gubbins, *Molec. Phys.*, **46**, 1109 (1982).
20. G.M. Torrie and J.P. Valleau, *Chem. Phys. Letters*, **28**, 587 (1974).
21. P.A. Lebowhl and G. Lasher, *Phys. Rev.*, **A6**, 426 (1972).
22. J.Y. Denham, R.L. Humphries and G.R. Luckhurst, *Molec. Cryst. Liq. Cryst. Letters.*, **41**, 67 (1977).
23. B.C. Freasier and L.K. Runnels, *J. Chem. Phys.*, **58**, 2963 (1973).
24. Habtamu Zewdie and G.R. Luckhurst, Unpublished work.
25. J.A. Barker and R.O. Watts, *Chem. Phys. Letters*, **3**, 144 (1969).
26. J.S. Rowlinson and B. Widom, "Molecular Theory of Capilarity", Clarendon Press, Oxford (1982).